New calculational scheme for particle range and an application to a positron entering a metal

J. Oliva*
University of California at San Diego, La Jolla, California 92093
(Received 13 August 1979)

A new scheme for evaluating the stopping distance of a particle in a uniform medium is presented. The input is the bulk (inelastic) differential transition probability per unit time of the particle in the medium. The range is determined as the mean penetration depth associated with all possible paths available to the particle in the course of its slow down. The totality of possible paths is represented approximately by means of a tree-type construction which takes account of the role of angular deflections. The rms deviation in the penetration depth is also given. The procedure is applied to a positron entering a metal. We find that for medium energies the range is determined principally by positron-conduction-electron scattering while the spread in penetration depths is limited by positron-phonon scattering. Results also show that for incident energies $\lesssim 25$ a.u. significant numbers of nonthermalized positrons reach the surface.

I. INTRODUCTION

We present in this paper a new general approximate procedure for the evaluation of the range (stopping distance) of a particle entering a homogeneous medium, e.g., a uniform many-body system. This scheme differs from others[1] mainly in the manner in which the angular deflection of the slowing particle is taken into account. The procedure is very simple to implement and, though having a recursive character, will often be amenable to hand calculation thereby offering a major advantage over more involved albeit more accurate numerical procedures, e.g., Monte Carlo simulation.

The input to the procedure is the bulk[2] differential transition probability from momentum state $\vec{p}$ to $\vec{p}'$ per unit time $\sigma(\vec{p},\vec{p}')$, for the particle in the given medium. This quantity is most conveniently identified as twice the magnitude of the integrand of an expression for the imaginary part of the self-energy Σ_I as an integral over momentum space:

$$\Sigma_I(\vec{p}) = \int f(\vec{p},\vec{p}')d^3p' \ , \tag{1a}$$

$$\sigma(\vec{p},\vec{p}') = 2|f(\vec{p},\vec{p}')| \ . \tag{1b}$$

Such expressions for Σ_I arise naturally out of many-body perturbation-theoretic approaches. We note that this identification of the differential transition probability rests upon the interpretation of Σ_I as proportional to the total transition rate of the particle in the medium. Such an interpretation is legitimate provided that the quasiparticle picture is valid. This will generally be the case in practice. As an example of the use of our procedure we conclude with a computation of the range of a positron entering a metal.[3]

II. GENERAL COMPUTATION SCHEME FOR RANGE

The total transition rate for a particle of momentum $\vec{p}$ in the given medium, $\dot{n}(\vec{p})$, is given by

$$\dot{n}(\vec{p}) = \int \sigma(\vec{p},\vec{p}')d^3p' \ . \tag{2}$$

In view of our interpretation of $\sigma(\vec{p},\vec{p}')$ the average time rate of change of energy $\dot{E}(\vec{p})$ and average time rate of change of angular deflection $\dot{\theta}(\vec{p})$ (where θ is the polar angle of deflection about the direction of $\vec{p}$) are expressible as

$$\dot{E}(\vec{p}) = \int \sigma(\vec{p},\vec{p}')[E(\vec{p}')-E(\vec{p})]d^3p' \ , \tag{3}$$

$$\dot{\theta}(\vec{p}) = \int \sigma(\vec{p},\vec{p}')\theta(\vec{p}')d^3p' \ , \tag{4}$$

where

$$E(\vec{p}) = \frac{p^2}{2m} \ , \tag{5}$$

$$\theta(\vec{p}) = \cos^{-1}\left(\frac{\vec{p}\cdot\vec{p}'}{pp'}\right) \ . \tag{6}$$

For a homogeneous system, $\dot{\theta}(\vec{p})$ is independent of the direction of $\vec{p}$.

Using Eqs. (2), (3), and (4), we arrive at the following expressions for the mean energy change per collision $dE(\vec{p})/dn$ and the mean angular deflection per collision $d\theta(\vec{p})/dn$:

$$\frac{dE(\vec{p})}{dn} = \frac{\int \sigma(\vec{p},\vec{p}')[E(\vec{p}')-E(\vec{p})]d^3p'}{\int \sigma(\vec{p},\vec{p}')d^3p'} \tag{7}$$

$$\frac{d\theta(\vec{p})}{dn} = \frac{\int \sigma(\vec{p},\vec{p}')\theta(\vec{p}')d^3p'}{\int \sigma(\vec{p},\vec{p}')d^3p'} \tag{8}$$

Finally, the mean free path between collisions is given by

$$\lambda(\vec{p}) = \frac{[2mE(\vec{p})]^{1/2}}{\int \sigma(\vec{p},\vec{p}')d^3p'} , \tag{9}$$

while the mean collision time is given by

$$\tau(\vec{p}) = \frac{1}{\int \sigma(\vec{p},\vec{p}')d^3p'} . \tag{10}$$

We now introduce a geometric construction which corresponds to the totality of possible paths taken by a particle entering a uniform medium in the course of its slowing down and coming to thermal equilibrium. Recall that our main purpose here is the determination of the mean depth of penetration of a particle entering the system. As such we will be concerned with computing the average component in the direction normal to the interface (assuming normal incidence) of all position vectors corresponding to the endpoints of all possible paths taken by the thermalizing particle.

We take the point of view that the thermalization proceeds as a discrete succession of scatterings, each scattering separated in time by the (energy-dependent) mean collision time. The chain of scatterings ends when the particle energy has been degraded to thermal energies. Of course as the particle slows down it suffers angular deflection which in the case of a positron entering a metal will be shown to be quite significant during the most important phase of the thermalization process, namely, that associated with the slow down from a few tenths the Fermi energy to thermal energies. In this range of energies the mean free path is quite large and therefore strong diffuse scattering will play an important role in reducing the mean penetration. A calculation of range must therefore take proper account of angular deflection.

The construction mentioned above is shown in Fig. 1. The particle enters the system at energy E_0. It travels a distance $\lambda_0 \equiv \lambda(E_0)$ without deflection. It then undergoes its "first" collision whereupon it loses an energy ΔE_1, taken as the mean energy loss per collision at the energy E_0:

$$\Delta E_1 = \left.\frac{dE}{dn}\right|_{E=E_0} \tag{11}$$

[see Eq. (7)]. In addition, the particle will undergo an angular deflection θ_1 which is taken to be the mean angular deflection per collision at the energy E_0:

$$\theta_1 = \left.\frac{d\theta}{dn}\right|_{E=E_0} . \tag{12}$$

The particle is allowed to scatter with any azimuthal angle around the original direction of momentum. The particle then travels undeviated a distance

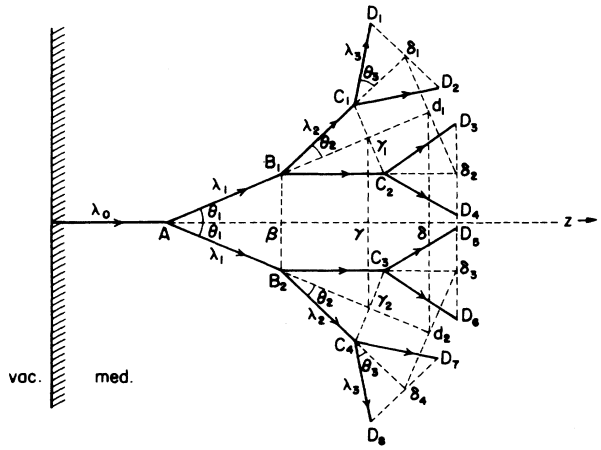

FIG. 1. Tree of possible paths available to particle up to fourth scattering. This is a 2D cross section showing only links on those 3D cones which have vertices in the plane of the paper. $\beta\gamma$ is the mean incremental advance Δz_2 due to the four 2 links shown and to all other 2 links (i.e., all remaining ones on the cones with vertices at B_1 and B_2 and all those on all other 2 cones centered on the rim of the 1 cone). Similarly $\gamma\delta$ is the mean incremental advance Δz_3 due to the eight 3 links shown and to all other 3 links. The particle energy drops at each node and the tree continues until the energy has degraded to thermal energies.

$\lambda_1 \equiv \lambda(E_1)$ with

$$E_1 \equiv E_0 + \Delta E_1 , \tag{13}$$

i.e., a distance equal to the mean free path at the reduced energy.

Thus, within this model up to the second collision [i.e., after the total path length is $\lambda(E_0)+\lambda(E_1)$] there is an infinite number of possible paths available to the particle each of which is comprised of the original undeviated link of length λ_0 plus a link of length λ_1 (the "1 link") lying on the surface of a cone (the "1 cone") having apex angle θ_1, side λ_1, and axis parallel to the original momentum. Referring to Fig. 1 (which is a two-dimensional cross section of the three-dimensional tree of paths chosen such that only the two-dimensional cross sections of those cones with vertices in the plane of the paper are shown), the mean penetration in the z direction $\bar{z}_2$ just before the second collision is clearly given by

$$\bar{z}_2 = \lambda_0 + \lambda_1 \cos\theta_1 . \tag{14}$$

After the particle has traveled a distance λ_1 along the first cone, it scatters a second time, loses an energy

$$\Delta E_2 = \left.\frac{dE}{dn}\right|_{E=E_1} , \tag{15}$$

and suffers an angular deflection θ_2 given by

$$\theta_2 = \left.\frac{d\theta}{dn}\right|_{E=E_1} . \tag{16}$$

Note that these changes in energy and angle are evaluated using the reduced energy E_1 along the 1 link. Now each point on the rim of the 1 cone gives rise in turn to a new cone of possible 2 links each with the same apex angle θ_2 (due to the homogeneity of the system) and with axis parallel to the side of the 1 cone. From Fig. 1 it is clear that the mean incremental advance in the z direction arising from all 2 links is the z component of the vector mean of the vector means of all vectors along the surface of each 2 cone. That is, the mean incremental advance arising from all 2 links is the z component of the mean of all vectors of the type $B_i\gamma_i$, each of these in turn being the mean of all vectors of the type B_iC_j. Now clearly, $B_i\gamma_i = \lambda_2\cos\theta_2$. The mean of all vectors of the type $B_i\gamma_i$ is $\beta\gamma$, given by $B_i\gamma_i\cos\theta_1$,. and is equal to its z component. Thus the mean incremental advance, Δz_2, in the z direction arising from all 2 links is given by

$$\Delta z_2 = \lambda_2\cos\theta_2\cos\theta_1 \ , \tag{17}$$

and the mean net advance in the z direction $\bar{z}_3$ just before the third collision is given by [using Eqs. (14) and (17)]

$$\bar{z}_3 = \lambda_0 + \lambda_1\cos\theta_1 + \lambda_2\cos\theta_2\cos\theta_1 \ . \tag{18}$$

The pattern is now apparent and it is straightforward to induce the following result for the mean net advance $\bar{z}_n$ in the z direction just before the occurrence of the nth collision:

$$\bar{z}_n = \sum_{i=0}^{n-1}\lambda_i\prod_{j=0}^{i}\cos\theta_j \ , \tag{19}$$

where $\theta_0 = 0$. Entering in Eq. (19) are the energy-dependent mean free paths

$$\lambda_i = (2mE_i)^{1/2}\tau(E_i) \ , \tag{20}$$

and energy-dependent mean scattering angle per collision

$$\theta_i = \left.\frac{d\theta}{dn}\right|_{E=E_{i-1}} \ , \tag{21}$$

with the set of link energies E_i satisfying

$$E_i = E_{i-1} + \Delta E_i \ , \tag{22a}$$

$$\Delta E_i = \left.\frac{dE}{dn}\right|_{E=E_{i-1}} \ , \tag{22b}$$

with E_0 = incident energy.

The range is given by $\bar{z}_{n_r}$ where n_r is chosen such that E_{n_r} is less than the thermal energy ($\frac{3}{2}k_BT$) while E_{n_r-1} is greater than the same. It will turn out that for a positron entering a metal, the range will be independent of the specific choice of n provided it is near n_r, the reason being that in general the scattering will be sufficiently diffuse well before the energy has degraded to thermal energies that the mean incremental advance in the normal direction due to all n links with $n \approx n_r$ will be negligible.

Two remarks are in order concerning the averaging procedure by which the angular deflection has been taken into account. We first note that the above scheme yields consistent results for range in the limit where the angular deflections per collision are extremely small throughout the slow down (pure forward-scattering limit). In that case, the particle moves along a straight line and, again regarding the slow down process as a discrete succession of scatterings, it is clear that the range is given by $R = \sum_{i=0}^{n_r-1}\lambda_i$. The general result, Eq. (19) conforms to this when $\theta_i = 0$, $i = 0, \ldots n_r - 1$. Going to the opposite limit of extreme diffuse scattering it is again true that the reasoning employed above yields a consistent result. For example, let us suppose that $\theta_i = \frac{1}{2}\pi$, $i = m, m+1, \ldots, m'$. It is immediately clear from the construction of Fig. 2 that the mean incremental advance associated with this set of links is zero and that therefore there is no net penetration of the particle.

We finally determine the root-mean-square deviation σ_n from the mean penetration $\bar{z}_n$. It is straightforward but rather tedious (the proof is analogous to the preceding derivation of $\bar{z}_n$) to obtain the following result by induction:

$$\sigma_n = \begin{cases} 0, & n < 3 \ , \\ \left(\frac{1}{2}\sum_{m=1}^{n-2} S_{m,n}^2\sin^2 A_{m,n}\sin^2\theta_{n-m}\right)^{1/2}, & n \geq 3 \ , \end{cases} \tag{23}$$

where the $S_{m,n}$ are generated by

$$\begin{aligned} S_{m,n} &= \cos\theta_{n-m+1}S_{m-1,n} + \lambda_{n-m} \ , \\ S_{0,n} &= 0 \ , \end{aligned} \tag{24}$$

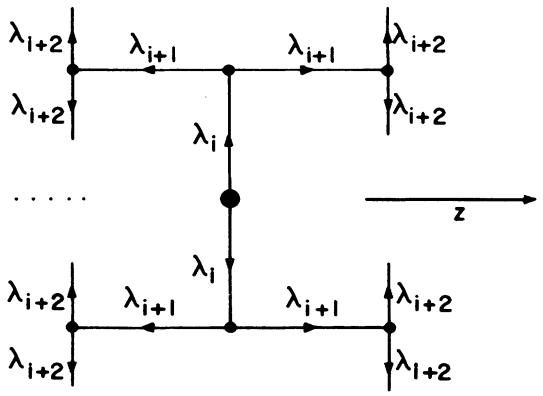

FIG. 2. Branch of tree construction corresponding to extreme diffuse scattering limit. Note net advance in z direction associated with any set of n links shown is zero though spreading of cloud of possible trajectories continues.

and where

$$A_{m,n} = \sum_{i=1}^{n-m-1} \theta_i \tag{25}$$

In order that our interpretation of z_{n_r} as a range of a particle entering a medium with a surface at $z=0$ be reasonable it is necessary that

$$\sigma_n < \bar{z}_n, \quad n = 1, 2, \ldots, n_r \ , \tag{26}$$

i.e., that the "cloud" of possible trajectory endpoints not extend to the surface. This will generally be true for higher energies.

III. APPLICATION: RANGE OF A POSITRON ENTERING A METAL

We calculate the range of a positron entering a metal using the above theory. We take into account both positron–conduction-electron and positron-phonon scattering. Although in general it is not clear how important elastic ion-core scattering is in determining the stopping distance, it is neglected here as a first approximation. It should be noted, however, that since (as will be seen) the mean penetration depth is determined in this approximation mainly by the slow down from the incident energy (typically a few keV) to ~ 100 eV and that since the core elastic scattering at these energies is (as is electron and phonon inelastic scattering) rather peaked in the forward direction (forward *elastic* scattering does not give a finite stopping depth) and is occurring at a rate comparable to the electron plus phonon scattering rate,[4] our results are probably accurate to within $\sim 25\%$ within the overall tree construction framework.

The starting point is Eq. (19) which when evaluated at $n = n_r$ gives the mean penetreation depth to thermalization. We require the energy-dependent mean free paths λ_i [Eq. (20)] and energy-dependent mean scattering angles per collision θ_i [Eq. (21)] which in turn require the mean energy losses per collision ΔE_i [Eqs. (22) and (7)].

Positron–conduction-electron scattering has been discussed at some length in an earlier paper.[5] Given there is an expression for the imaginary part of the positron self-energy from which we are able to identify

$$\sigma_{\rm el}(\vec{p}, \vec{p}-\vec{k}) = \begin{cases} \dfrac{e^2}{\pi^2 k^2} \left| \mathrm{Im} \dfrac{1}{\epsilon_{\rm RPA}(k, E(p) - E(\vec{p}-\vec{k}) + i\delta)} \right|, & 0 < E(\vec{p}-\vec{k}) < E(p), \\ 0, \quad \text{otherwise}, \end{cases} \tag{27}$$

where e is the electron charge and $\epsilon_{\rm RPA}(k, \omega)$ is the wave-number and frequency-dependent Lindhard dielectric function.

Positron-phonon scattering has been evaluated (within the Debye model) by Perkins and Carbotte[6] who give an expression for the phonon contribution to the imaginary part of the positron self-energy from which we can identify (with the introduction here of a Debye cutoff factor)

$$\sigma_{\rm ph}(\vec{p}, \vec{p}-\vec{k}) = \frac{\gamma^2}{4\pi^2} k\, \delta(E(p) - \omega(k) - E(\vec{p}-\vec{k})) \times \theta(\omega_D - \omega(k)) \ , \tag{28}$$

where $\omega(k) = ck$, with c the speed of sound, $\omega_D = ck_D$ is the Debye frequency, and γ is the positron-phonon coupling constant.[7] The total differential transition probability for the positron in the metal is taken as $\sigma_{\rm tot} = \sigma_{\rm el} + \sigma_{\rm ph}$. It was shown in Ref. 5 that

$$\dot{n}_{\rm el}(E) = \begin{cases} \dfrac{\pi e^2 m a_0}{15 E_F} E^2, & E \ll E_F \ , \\ \dfrac{m^{1/2} e^2 \omega_0}{2^{3/2} E^{1/2}} \ln\left(\dfrac{E}{E_F}\right), & E \gg E_F \ , \end{cases} \tag{29}$$

where m is the positron mass, a_0 the Bohr radius, E_F the Fermi energy, and ω_0 the plasma frequency. Using Eqs. (2) and (28), we find

$$\dot{n}_{\rm ph}(E) = \frac{\gamma^2 m^{1/2}}{6\sqrt{2}\pi E^{1/2}} \times \begin{cases} 8[(2mE)^{1/2} - mc]^3, & E < \dfrac{1}{2m}(\tfrac{1}{2}k_D + mc)^2 \ , \\ k_D^3, & E > \dfrac{1}{2m}(\tfrac{1}{2}k_D + mc)^2 \ . \end{cases} \tag{30}$$

We thus see that at low energies the phonon scattering dominates the total collision rate $\dot{n}(E)$. In fact, at thermal energies ($\frac{3}{2}k_B T$) with $T = 300$ K (1000 K) we find for the case of Al $\dot{n}_{\rm ph} = 1.0 \times 10^{-4}$ a.u. (3.8×10^{-4} a.u.) and $\dot{n}_{\rm el} = 9.2 \times 10^{-7}$ a.u. (4.6×10^{-6} a.u.); i.e., $\dot{n}_{\rm ph}$ is about two orders of magnitude larger than $\dot{n}_{\rm el}$. On the other hand, for larger energies $\dot{n}$ is dominated by $\dot{n}_{\rm el}$. Figure 3 is a plot of mean free path versus energy for Al allowing for both positron-phonon and positron–conduction-electron scattering.

We note

$$\lambda(E) \sim \frac{1}{E^{1/2}}, \quad E << E_F \tag{31}$$

We next evaluate the time rate of energy loss $\dot{E}(E) = \dot{E}_{el}(E) + \dot{E}_{ph}(E)$. Using Eqs. (3) and (27), it can be shown that

$$\dot{E}_{el}(E) = \begin{cases} -\frac{4\pi e^2 m a_0}{105 E_f} E^3 \sim E^3, & E << E_F \ , \quad (32a) \\ -\frac{e^2 \omega_0^2 m^{1/2}}{2^{3/2} E^{1/2}} \ln\left(\frac{E}{E_F}\right) \sim \frac{1}{E^{1/2}} \ln E, & E >> E_F \ . \quad (32b) \end{cases}$$

For $\dot{E}_{ph}(E)$, using Eq. (28) it is found[8]

$$\dot{E}_{ph}(E) = -\frac{\gamma^2 m^{1/2} c}{8\sqrt{2}\pi E^{1/2}} \begin{cases} 16[(2mE)^{1/2} - mc]^4 \sim E^{3/2}, & E < \frac{1}{2m}(\frac{1}{2}k_D + mc)^2 \ , \\ k_D^4 \sim \frac{1}{E^{1/2}}, & E > \frac{1}{2m}(\frac{1}{2}k_D + mc)^2 \ , \end{cases} \tag{33}$$

the $E^{3/2}$ behavior being valid provided $E >> \frac{1}{2}mc^2$. Positron-phonon scattering is thus the dominant mechanism for energy dissipation at typical thermal energies. The mean energy change per collision dE/dn is expressible as

$$\frac{dE}{dn} = \frac{\dot{E}_{el} + \dot{E}_{ph}}{\dot{n}_{el} + \dot{n}_{ph}} \ , \tag{34}$$

$$\frac{dE}{dn} \approx \frac{\dot{E}_{ph}}{\dot{n}_{ph}} = -\frac{3}{4}c \begin{cases} 2[(2mE)^{1/2} - mc], & E < \frac{1}{2m}(\frac{1}{2}k_D + mc)^2, \\ k_D, & E > \frac{1}{2m}(\frac{1}{2}k_D + mc)^2, \end{cases} \quad E << E_f \ , \tag{35}$$

$$\frac{dE}{dn} \approx \frac{\dot{E}_{el}}{\dot{n}_{el}} = -\omega_0, \quad E >> E_F \ , \tag{36}$$

i.e., at very high energies, each scattering is associated with the emission of a single plasmon. Numerical results for dE/dn for Al in the entire energy range appear in Fig. 4.

Finally, we evaluate the time rate of change of scattering angle $\dot{\theta}(E)$ ($\dot{\theta} = \dot{\theta}_{el} + \dot{\theta}_{ph}$). In view of Eqs. (4), (27), and (28) we need the angular deviation $\theta(\vec{k})$ associated with a virtual scattering as function of the momentum transfer $\vec{k}$. Now $\theta(\vec{k})$ is the angle made by the virtual final-state momentum $\vec{p}' = \vec{p} - \vec{k}$ with respect to the direction of p. We obtain

$$\theta(k,x) = \sin^{-1}\left[\frac{k(1-x^2)^{1/2}}{(p^2 + k^2 - 2pkx)^{1/2}}\right] \ , \tag{37}$$

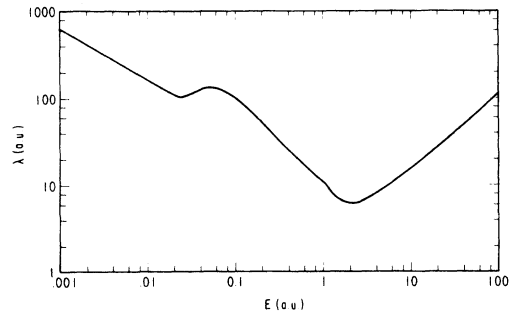

FIG. 3. Positron mean free path vs energy in Al (positron–conduction-electron and positron-phonon scattering taken into account; $T = 0$).

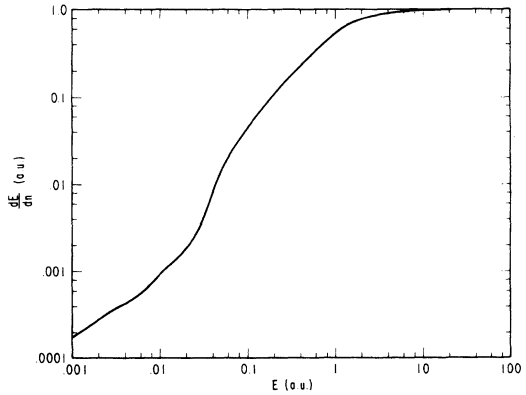

FIG. 4. Mean energy loss per collision vs energy for a positron in Al (positron–conduction-electron and positron-phonon scattering taken into account; $T = 0$).

where x is the cosine of the angle between $\vec{p}$ and $\vec{k}$. Results of numerically integrating Eq. (4) using Eqs. (27) and (37) show that $\dot{\theta}_{el}(E) \sim E^2$ for $E << E_F$. Using Eqs. (28) and (37) in Eq. (4), and changing variables to $\theta(k,x(k))$ in the $|k|$ integration gives after some algebra

$$\dot{\theta}_{ph}(E) = \frac{\gamma^2 8m^2 E}{3\pi}\left(\pi - \tfrac{4}{3}\right) \sim E \ , \quad \tfrac{1}{2}mc^2 << E << \tfrac{1}{4}\left(\frac{k_D^2}{2m}\right) \ . \tag{38}$$

Again, phonon scattering dominates at low energies. We find

$$\frac{d\theta}{dn} \approx \frac{\dot{\theta}_{ph}}{\dot{n}_{ph}} \sim \pi - \tfrac{4}{3}, \quad \tfrac{1}{2}mc^2 << E << \tfrac{1}{4}\left(\frac{k_D^2}{2m}\right) \ . \tag{39}$$

Plots of $d\theta/dn$ for Al obtained numerically over the full energy range appear in Fig. 5. We note that the slight nonanalytic kink noticeable at $E \approx 1.16$ a.u. in the λ, dE/dn, and $d\theta/dn$ vs E curves arises from the onset of plasmon excitation.

We are thus now able to generate the E_i's of Eq. (22) and in turn, the θ_i's and λ_i's of Eqs. (21) and (20). Results for range versus energy for Al appear in Fig. 6. The results are insensitive to temperatures within the range $T = 300$–900 K.[9] The rms deviation from the mean penetration depth also appears in Fig. 6. These results indicate that the minimum incident energy required in order that most positrons thermalize prior to escape is ~ 25 a.u. For lower energies, an increasing fraction of particles will reach the surface and escape prior to thermalization. Thus our results for range are valid in the intermediate energy range and above ($E > \sim 25$ a.u.).

Returning to the medium energy case, we point out that our calculational scheme provides us with more information than just range and dispersion. By examining the successive values of $\bar{z}_n$ and σ_n as function of the mean collisioin number n we are in fact able to follow the entire development of the slowing cloud of particles. Plots of $\bar{z}_n$ and $\bar{\sigma}_n$ for a representative case

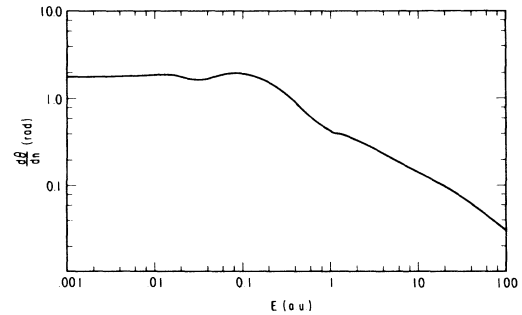

FIG. 5. Mean angular deflection per collision vs energy for a positron in Al (positron–conduction-electron and positron-phonon scattering taken into account; $T = 0$).

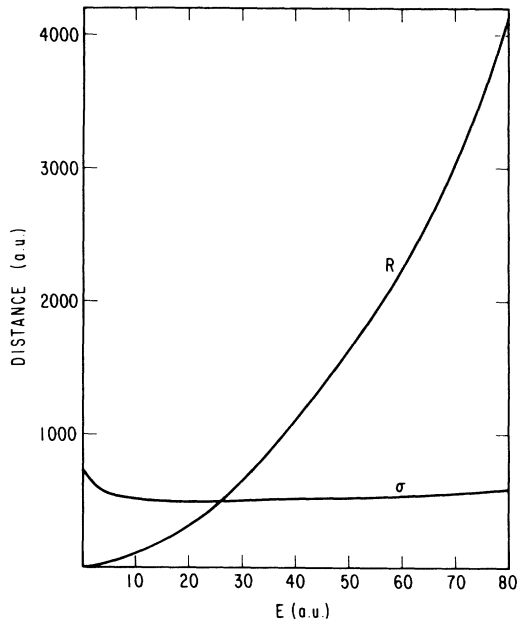

FIG. 6. Range R and rms deviation in range σ vs energy for a positron entering Al (positron–conduction-electron and positron-phonon scattering taken into account; $T = 0$). The intersection at $E \approx 25$ a.u. indicates that most particles thermalize before returning to the surface for $E \gtrsim 25$ a.u.

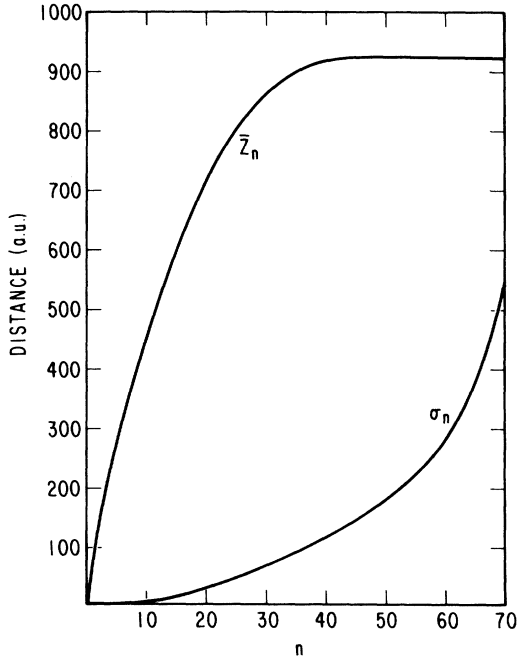

FIG. 7. Mean penetration depth $\bar{z}_n$ and dispersion σ_n vs mean collision number for a 35 a.u. positron beam incident on Al. $\bar{z}_n$ saturates at $n \approx 35$ while σ_n continues to grow. This indicates complete randomization of velocity direction and increasing spread of the slowing cloud of positrons.

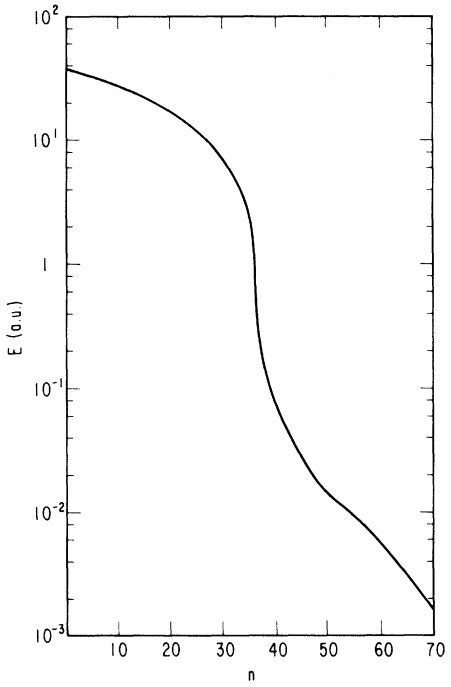

FIG. 8. Energy vs mean collision number for a 35 a.u. positron beam incident on Al.

($E = 35$ a.u.) appear in Fig. 7 while E vs n appears in Fig. 8. We notice that the range begins to saturate at about $n \approx 35 (E \approx 2$ a.u.); i.e., there is essentially no net further advance of the centroid of the cloud of particles by the time the mean particle energy has degraded to $E \approx 2$ a.u. This of course means that by the time the mean particle energy has dropped to this level, the directions of all particles have been completely randomized. Note however that the rms deviation continues to grow beyond $n \approx 35$ until thermalization is complete. This manifests the expected spreading in the by now diffuse cloud of particles. We observe further that for this medium high incident energy, $\sigma_n < \bar{z}_n$ for all n; i.e., the cloud is confined to the interior of the metal throughout the slow down.

The saturation in range occurs before the positron energy has degraded to the point where the positron-phonon interaction is important ($E \sim 0.2$ a.u. for Al). Thus the positron-electron scattering is the primary determinant of the range for energies $E \gtrsim 35$ a.u. (for Al). The phonons do play a role however in reducing the rms deviation in the range during the final stages of the thermalization since they reduce the mean free path by two orders of magnitude (while still giving rise to large angular deflections). This reduction is significant since the positron-electron mean free path is $\sim 10^4$–10^5 a.u. for thermal energies and thus considerably greater than the range in the ~ 30–50 a.u. regime.

Generalization of the above ansatz to the more realistic case where the particle is allowed to scatter into more than one polar angular channel and to travel any one of a number of different path lengths at each scattering node [with the distribution in polar angles and path lengths determined by the current value of (i.e., link) energy] will be the subject of a future publication.

ACKNOWLEDGMENTS

The author thanks Professor W. Kohn for a useful conversation and gratefully acknowledges the support of ONR through Contract No. N00014-76-C.

---

*Present address: Laboratory of Atomic & Solid State Physics, Cornell University, Ithaca, N.Y. 14853.

[1]For a review, see H. E. Schiott, in *Interaction of Energetic Charged Particles with Solids* (Brookhaven National Laboratory, Upton, N.Y., 1971).

[2]We ignore the smooth transition at the surface from bulk to vacuum behavior in the differential transition probability and moreover ignore any surface reflection effects. These approximations are quite legitimate for sufficiently high incident energies.

[3]Knowledge of the range of a positron entering a metal appears to be important [J. Oliva, (unpublished)] for an understanding of the recently observed [A. P. Mills, Jr., Phys. Rev. Lett. 41, 1828 (1978)] positronium formation process occurring outside metals being bombarded with medium-energy positrons.

[4]J. B. Pendry, *Low Energy Electron Diffration* (Academic, London, 1974), Chap. II.

[5]J. Oliva (unpublished).

[6]A. Perkins and J. P. Carbotte, Phys. Rev. B 1, 101 (1970).

[7]$\gamma^2 = (z^2 e^4 \pi^2 / \lambda^4)\ (8n/Mc)$ where z is the valence, n the ion density, M the ion mass, and λ the reciprocal Thomas-Fermi screening length for the electrons.

[8]The first of Eqs. (33) was obtained in Ref. 6.

[9]That is to say, independent of the choice of n_r over a corresponding range, i.e., the velocity directions have been completely randomized well before thermalization is complete, and the final stages of the thermalization do not advance the centroid of the slowing cloud of particles. (This observation justifies the neglect of finite-temperature effects in the evaluation of the self-energies.)